Journal of Materials Chemistry

Dynamic Article Links

Cite this: J. Mater. Chem., 2012, 22, 18433

www.rsc.org/materials

PAPER

Material solubility and molecular compatibility effects in the design of fullerene/polymer composites for organic bulk heterojunction solar cells†

Pavel A. Troshin,*[a] Diana K. Susarova,[a] Ekaterina A. Khakina,[a] Andrey A. Goryachev,[a] Oleg V. Borshchev,[b] Sergei A. Ponomarenko,[b] Vladimir F. Razumov[a] and N. Serdar Sariciftci[c]

Received 7th May 2012, Accepted 22nd June 2012
DOI: 10.1039/c2jm32873a

We report a systematic study of more than 100 bicomponent systems composed of 19 different fullerene derivatives blended with 9 different conjugated polymers (including previously investigated poly(3-hexylthiophene)). It was shown that short circuit current density (J_{SC}) and light power conversion efficiency (η) of the fullerene/polymer photovoltaic devices depend on the solubility of the fullerene components in the solvent used for the blend film deposition (chlorobenzene). The revealed dependences have unusual "double branch" character because many fullerene derivatives possessing similar solubilities showed different photovoltaic performances. This behavior was related to the peculiarities of the molecular structures of the fullerene derivatives. Substituents attached to the cyclopropane ring fused with the fullerene cage in methanofullerenes affected both the morphology of their composites with conjugated polymers and their photovoltaic performance. It was demonstrated that variation of the fullerene component blended with a conjugated polymer might easily change its photovoltaic performance by a factor of 3–4. The obtained results proved that design of appropriate fullerene derivatives and novel conjugated polymers are equally important tasks on the way towards highly efficient organic photovoltaics.

Introduction

Organic photovoltaics is a rapidly progressing field nowadays demonstrating fullerene/polymer and fullerene/small molecule solar cells with efficiencies approaching the level of 7–9%.[1] Major breakthroughs are associated with the development of novel electron donor materials, particularly, low band gap conjugated polymers.[2,3] Even though the design rules were formulated for conjugated polymers,[4] their development is mainly progressing through empirical screening.[5,6] Many conjugated polymers possessing optimal electronic properties failed to give expected high photovoltaic efficiencies.[7–9] Unfortunately, the factors responsible for unsatisfactory characteristics of some polymers usually remain unclear. It is quite probable that poor photovoltaic performance is not an inherent characteristic of a polymer but is related to the unsatisfactory properties of the second component (fullerene derivative) or unbalanced morphology of the blend.

It is somewhat surprising that fullerene derivatives have not been developed as intensively as conjugated polymers.[10,11] There are many fullerene-based materials that were designed and investigated in combination with some conventional polymers such as poly(3-hexylthiophene) (P3HT), poly[{2-methoxy-5-[3′-7′-dimethyloctyloxy]-1,4-phenylene}-1,2-ethenediyl] (MDMO-PPV) or poly[{[(2-ethylhexyl)oxy]methoxy-1,4-phenylene}-1,2-ethenediyl] (MEH-PPV).[12–19] In contrast, new generations of conjugated polymers are studied almost exclusively using [60]PCBM[20] and [70]PCBM[21] as electron acceptor counterparts.

We have designed recently a library of fullerene derivatives and performed their systematic investigation in bulk heterojunction solar cells in combination with P3HT.[22] It was revealed that physical properties of the fullerene-based compounds, such as their solubility in organic solvents, affect severely the photovoltaic performance of their composites with P3HT. Most importantly, good photovoltaic performance of P3HT was reached only using fullerene derivatives with optimal solubility. Fullerene-based materials with unsuitable (too high or too low) solubility yielded poor performance in solar cells with P3HT.

If the trend revealed for P3HT is also valid for other conjugated polymers, it might explain why many polymers with advanced electronic properties failed to give highly efficient solar cells in combination with PCBM. In order to check this hypothesis in this work we investigated systematically several different conjugated polymers combining each of them with a series of fullerene derivatives with variable solubility.

[a]*Institute for Problems of Chemical Physics of Russian Academy of Sciences, Semenov Prospect 1, Chernogolovka, Moscow region, 142432, Russia. E-mail: troshin2003@inbox.ru*
[b]*Enikolopov Institute of Synthetic Polymeric Materials, Russian Academy of Sciences, 70 ul. Profsoyuznaya, 117393 Moscow, Russia*
[c]*Linz Institute for Organic Solar Cells (LIOS), Johannes Kepler University Linz, Altenbergerstrasse 69, A-4040 Linz, Austria*
† Electronic supplementary information (ESI) available. See DOI: 10.1039/c2jm32873a

Results and discussion

1. The molecular structures of the materials

The molecular structures of the materials involved in the present study are shown in Fig. 1. The fullerene components are represented by cyclopropane derivatives of C_{60} and C_{70} called in general "methanofullerenes". The examples of such fullerene derivatives are known in the literature as [60]PCBM and [70]PCBM. The synthesis of all fullerene derivatives was performed in accordance with the previously reported procedure. Detailed descriptions of the syntheses and spectral characteristics of the specific methanofullerenes were reported previously.[15,23–25]

Many of the presented fullerene derivatives were studied previously in photovoltaic devices in combination with P3HT. From the series of 27 different fullerene derivatives reported earlier we intentionally excluded compounds with solubilities in chlorobenzene below 17 mg ml^{-1} because of their poor performance in photovoltaic devices. In addition to this selection we prepared some compounds possessing solubilities in chlorobenzene equal to or higher than 17 mg ml^{-1} (**F6**, **F15–F18**). We note that all fullerene derivatives used in the present study possess almost identical reduction potentials (implying that they have very similar LUMO energy levels). Therefore, differences in the electronic properties of various fullerene derivatives and influence of such differences on photovoltaic performance might be kept out of consideration in this study.

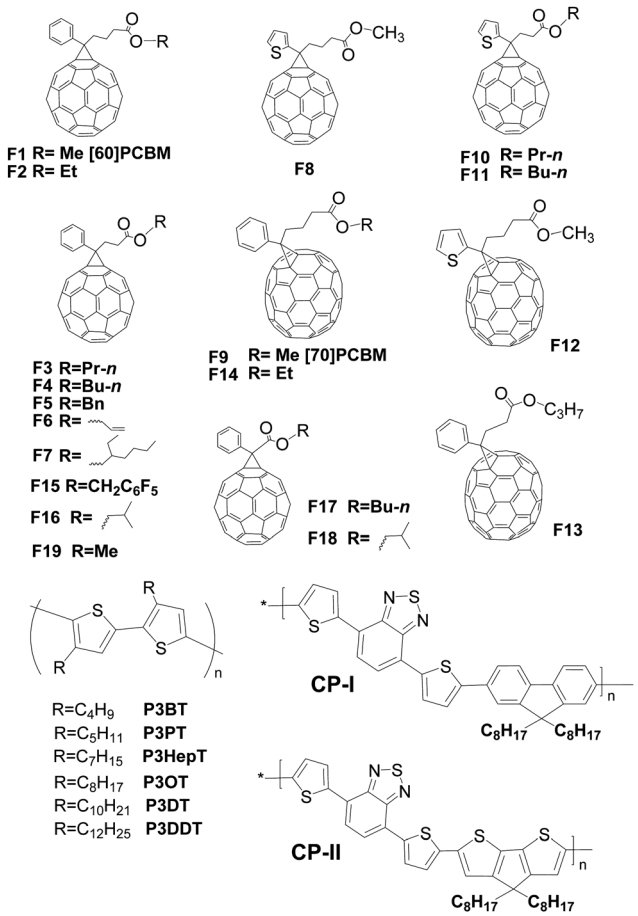

Fig. 1 Molecular structures of the investigated materials.

Poly(3-alkylthiophenes) with different alkyl side chains attached to the polythiophene backbone were first selected as electron donor components since they resemble P3HT which was investigated previously. In addition, we studied two electron donor copolymers. Copolymer poly[(9,9-dioctylfluorenyl-2,7-diyl)-alt-5,5-(4′,7′-di-2-thienyl-2′,1′,3′-benzothiadiazole)] (**CP-I**) was selected because of its high oxidation potential (deep lying HOMO energy level) enabling high open circuit voltages in photovoltaic devices with PCBM. Copolymer poly[(4,4-dioctyl-4H-cyclopenta[2,1-b:3,4-b′]dithiophene-2,6-diyl)-alt-5,5-(4′,7′-di-2-thienyl-2′,1′,3′-benzothiadiazole)] (**CP-II**) was selected because it is a low band gap material which should potentially produce high photocurrent densities in bulk heterojunction solar cells.[4]

2. Effect of the P3AT side chains on the morphology of their composites with the fullerene derivatives

It was shown previously that the length of alkyl side chains in poly(3-alkylthiophenes) (P3ATs) affects dramatically the morphology of their blends with [60]PCBM and their photovoltaic performance. Polymer with hexyl side chains (P3HT) was reported to be the optimal electron donor material among all investigated P3ATs.[26]

Here we monitored systematically the effect of the length of the side chains in P3ATs on the morphology and photovoltaic performance of their blends with different fullerene derivatives including [60]PCBM as a reference material. It was observed that polymer side chains indeed affect the morphology of all composites. Atomic force microscopy (AFM) images of the composites (annealed to reach the highest photovoltaic performance, see annealing regimes in Experimental) of fullerene derivative **F8** with different P3ATs are shown in Fig. 2. It is seen from the images that the composites of **F8** with P3PT, P3HT and P3HepT give rather smooth films with very similar surface topology. In contrast, P3ATs with shorter (P3BT) and longer (P3OT, P3DT and P3DDT) alkyl side chains produce much rougher films.

The composites of **F8** with P3OT, P3DT and P3DDT revealed characteristic features on the film surface implying a strong phase separation between the components in the blend. The existence of such phase separation was also confirmed by the phase AFM images (phase image for the **F8**/P3DDT is shown in Fig. 2H as an example). Very similar behavior was observed for the majority of all studied fullerene derivatives. The difference was only in the degree of the film surface coarsening going from one P3AT to the other. For example, the blends of P3ATs with fullerene derivative **F13** showed much smoother topologies compared to the analogous blends of **F8** (see Fig. S1 in the ESI†). Therefore, one might assume that **F13** induces smaller phase segregation in the blends with the polymers than the fullerene derivative **F8**. Other examples are provided by the blends of fullerene derivative **F3** with different P3ATs (Fig. S2†). The AFM images revealed that **F3** gives smooth and presumably rather homogeneous blends with all polythiophenes except for the ones with the shortest (P3BT) and the longest (P3DDT) side chains.

Thus, the presented examples proved that the film topology of the fullerene/P3AT blends depends on the length of the alkyl side chains attached to the polymer backbone. However, the film topology is also influenced significantly by the molecular

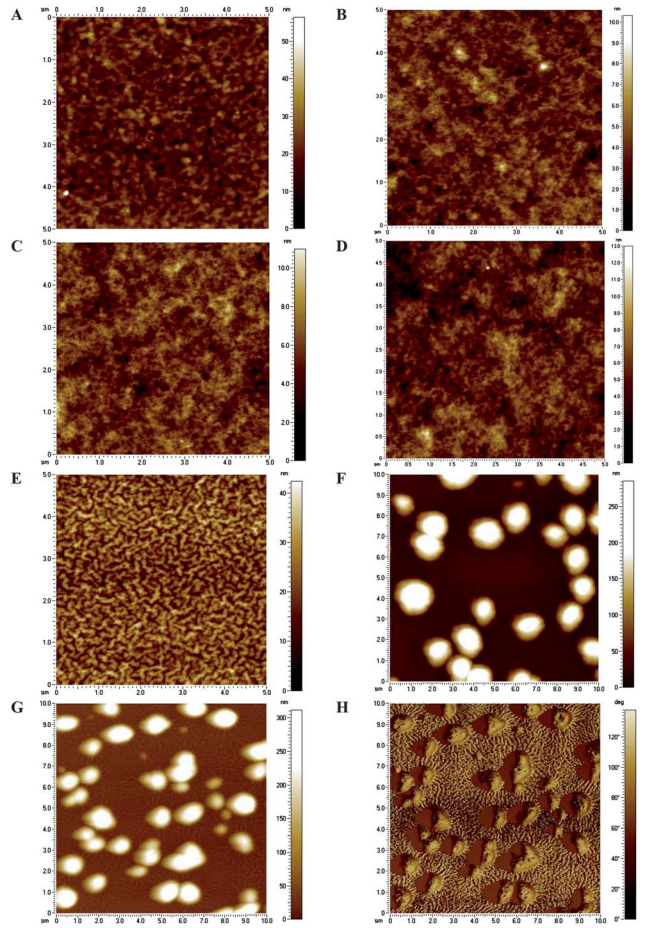

Fig. 2 AFM height images of the composites of **F8** with P3BT (A), P3PT (B), P3HT (C), P3HepT (D), P3OT (E), P3DT (F) and P3DDT (G). Phase image for the composite P3DDT (H) is provided as an additional illustration of the phase separation in the blend.

structure and physical properties of the fullerene derivative; these effects will be considered in more detail below.

3. Effect of the polymer side chains on the photovoltaic performance of their composites with the fullerene derivatives

Blending fullerene derivatives with P3ATs produced more than one hundred different fullerene/polymer composite systems that were investigated as photoactive layer materials in bulk heterojunction solar cells. The layout of a typical solar cell is shown schematically in Fig. 3.

It was demonstrated previously that composites of different P3ATs with [60]PCBM possess different morphologies and give different photovoltaic performances.[26] The best efficiencies were reached using P3HT as an electron donor polymer. Independent studies demonstrated that P3PT can give almost the same efficiency as P3HT in photovoltaic cells.[27,28] It was also noticed that open circuit voltage (V_{OC}) in photovoltaic devices increases with an increase in the length of the polymer side chains, especially when devices are built using pre-formed P3AT nanofibers,[29] Although poly(3-heptylthiophene) was investigated to a much lesser extent than P3PT, it can also be considered as a promising material for photovoltaic cells.[30]

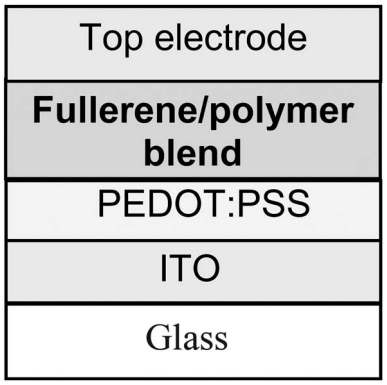

Fig. 3 Schematic layout of the organic photovoltaic cell.

In the present work we investigated the full series of P3ATs in combination with a set of different fullerene derivatives. For every fullerene derivative the characteristics of the photovoltaic cells were plotted as functions of the alkyl side chain length of the P3ATs used as electron donor counterparts (Fig. 4). The behavior of all studied fullerene derivatives is summarized in Fig. 4A. It is seen from the figure that the best power conversion efficiencies are reached in solar cells using P3PT and P3HT as electron donor polymers. The red line on the graph shows

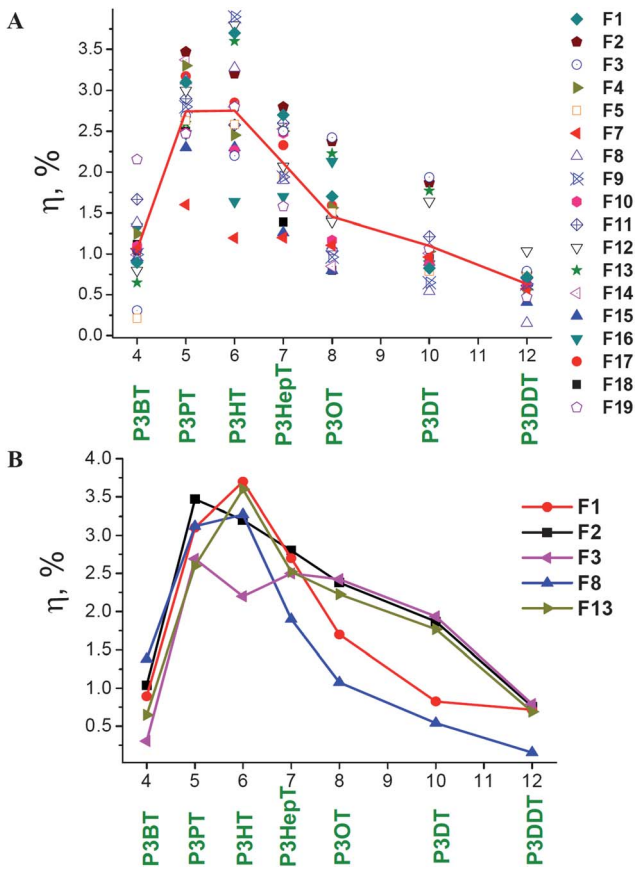

Fig. 4 The dependence of the light power conversion efficiency on the length of the P3AT side chains in devices comprising fullerene derivatives **F1–F19** (A); red line reflects the average photovoltaic performance of every P3AT with a certain alkyl chain length. Some selected dependences illustrate different behavior of various fullerene derivatives (B).

average efficiencies provided by each polymer blended with different fullerene derivatives. It is seen that P3HT and P3PT give equally high averaged performances, while other polymers demonstrate much lower efficiencies. Similar plots built for open circuit voltage (V_{OC}), short circuit current density (J_{SC}) and fill factor (FF) are presented in Fig. S3–S5 in the ESI.† Both J_{SC} and FF depend significantly on the length of the P3AT alkyl side chains. The character of these dependences resembles quite closely the shape of the efficiency–side chain length correlation shown in Fig. 4A. V_{OC} does not show any clear correlation with the structure of the P3AT used as electron donor component. This is an expectable result since V_{OC} usually depends on the energy levels of the materials and work functions of the electrodes that are very similar for the investigated systems.[31]

Different behavior of a few selected fullerene derivatives in composites with a series of P3ATs is illustrated in Fig. 4B. It is seen that **F1** ([60]PCBM), **F8** and **F13** give the peak performance in combination with P3HT as a donor component. In contrast, **F2** and **F3** yield the best performance in the blends with P3PT. The shapes of the efficiency–P3AT alkyl chain length profiles are different for the different fullerene derivatives. **F1** and **F8** demonstrate rapid decreases of the photovoltaic performance going from P3HT ($l = 6$) to P3HepT ($l = 7$) and then further to the polymers with the longer side chains. Fullerene derivatives **F2**, **F3** and **F13** show reasonably high performances with all P3ATs with except for the ones with the shortest (P3BT) and the longest (P3DDT) side chains.

The obtained results prove that photovoltaic performances of the fullerene/P3AT composites are governed by the lengths of the alkyl side chains attached to the polythiophene backbone. At the same time, molecular structure and properties of the fullerene component also affect significantly the photovoltaic performance of the P3AT/fullerene blends. The P3PT-based composite systems seem to be the least sensitive to the fullerene component. Longer alkyl chains attached to the polythiophene backbone increase the effect of the fullerene component on the photovoltaic performance of the polymer.

4. Influence of the solubility and peculiarities of the molecular structures of the fullerene derivatives on the photovoltaic performance of their composites with P3ATs

We reported previously that the photovoltaic properties of the fullerene/P3HT blends are governed mainly by the solubility of the applied fullerene derivatives in the solvents used for the active layer deposition.[22] Here we addressed the influence of the solubility of the fullerene derivatives on the photovoltaic performance of their blends with the whole series of P3ATs. Chlorobenzene was used as a solvent for the active layer deposition in the fabrication procedures of all photovoltaic devices presented in this work. The short circuit current density and power conversion efficiencies of the devices based on P3PT, P3HepT, P3OT and P3DT are plotted in Fig. 5 as functions of the solubility of the fullerene derivatives used as electron acceptor components in the blends. The analogues dependences for the V_{OC} and FF are shown in Fig. S6 in the ESI.† The plots for the systems comprising P3BT and P3DDT as donor polymers are given in Fig. S7.†

Considering the plots shown in Fig. 5 one might observe the appearance of two branches on the current density–solubility and efficiency–solubility profiles. These branches are formed as a result of splitting of all fullerene derivatives with the solubility lying in the range of 20–75 mg ml^{-1} into two groups.

Compounds forming the first group (upper-lying branch) showed significantly improved photovoltaic performance compared to the members of the second group (low-lying branch) even though they possess very similar solubilities in chlorobenzene. For example, compounds **F2** ($S = 19$ mg ml^{-1}) and **F14** ($S = 19$ mg ml^{-1}) show significantly higher light power conversion efficiencies in solar cells with P3PT or P3HepT polymers than compounds **F15** ($S = 20$ mg ml^{-1}), **F18** ($S = 17$ mg ml^{-1}) and **F19** ($S = 22$ mg ml^{-1}) possessing similar solubilities.

We emphasize that it is not correct to think that there are two well defined groups of fullerene derivatives that give low or high photovoltaic performance in combination with all investigated conjugated polymers. The situation might change significantly going from one polymer to the other for many fullerene derivatives. As an exception, the fullerene derivatives **F15** and **F18** showed inferior performance in solar cells regardless of the structure and properties of the polymer used as electron donor counterpart. However, many other fullerene derivatives behave in a different way. For instance, **F19** gives poor performance when combined with P3PT, P3HepT, P3OT and P3DT. In contrast, **F19**/P3DDT composite shows reasonably high efficiency. At the same time, compound **F19** outperforms all other fullerene derivatives in combination with P3BT. Other examples are provided by fullerene derivatives **F2** and **F14**. **F2** shows superior performance (upper branch on solubility profiles) in combination with all P3ATs except for P3BT. The compound **F14** works well in combination with P3PT and P3HepT, while its composites with other P3ATs showed inferior performances.

Finally, it is reasonable to consider fullerene derivatives **F8** ($S = 36$ mg ml^{-1}) and **F13** ($S = 35$ mg ml^{-1}) possessing very similar solubilities. Compound **F8** fits the upper branch on the solubility profile and gives better performance than **F13** (fits the lower branch) in solar cells with P3PT. However, the situation becomes opposite for the solar cells based on P3HepT. In that case **F13** outperforms **F8** significantly; therefore, **F13** fits the upper branch of the efficiency–solubility profile, while **F8** goes to the lower one. This illustrative example shows that the appearance of two branches on the efficiency–solubility profiles cannot be ascribed entirely to the molecular structure and properties of the fullerene derivatives. Most probably, such behavior originates from intermolecular interactions of the fullerene derivative and the polymer and is affected by the molecular structure and properties of both these components.

The fullerene derivative–polymer blend is a binary system whose morphology is determined by kinetic and thermodynamic factors. We believe that molecular structures of the materials govern both thermodynamics and kinetics of mixing and segregation of the polymer and fullerene components. It is known that an increase in the length of the solubilizing alkyl chains in poly(3-alkylthiophenes) changes the crystallinity of the polymer and also decreases its melting point and melting enthalpy significantly.[32] Introduction of branched side chains (*e.g.* 2-ethylhexyl) results often in the formation of amorphous polymers. These examples illustrate that solubilizing side chains affect the interchain (or intermolecular) interactions in the polymer. Very similar effects can be observed also for the fullerene derivatives.

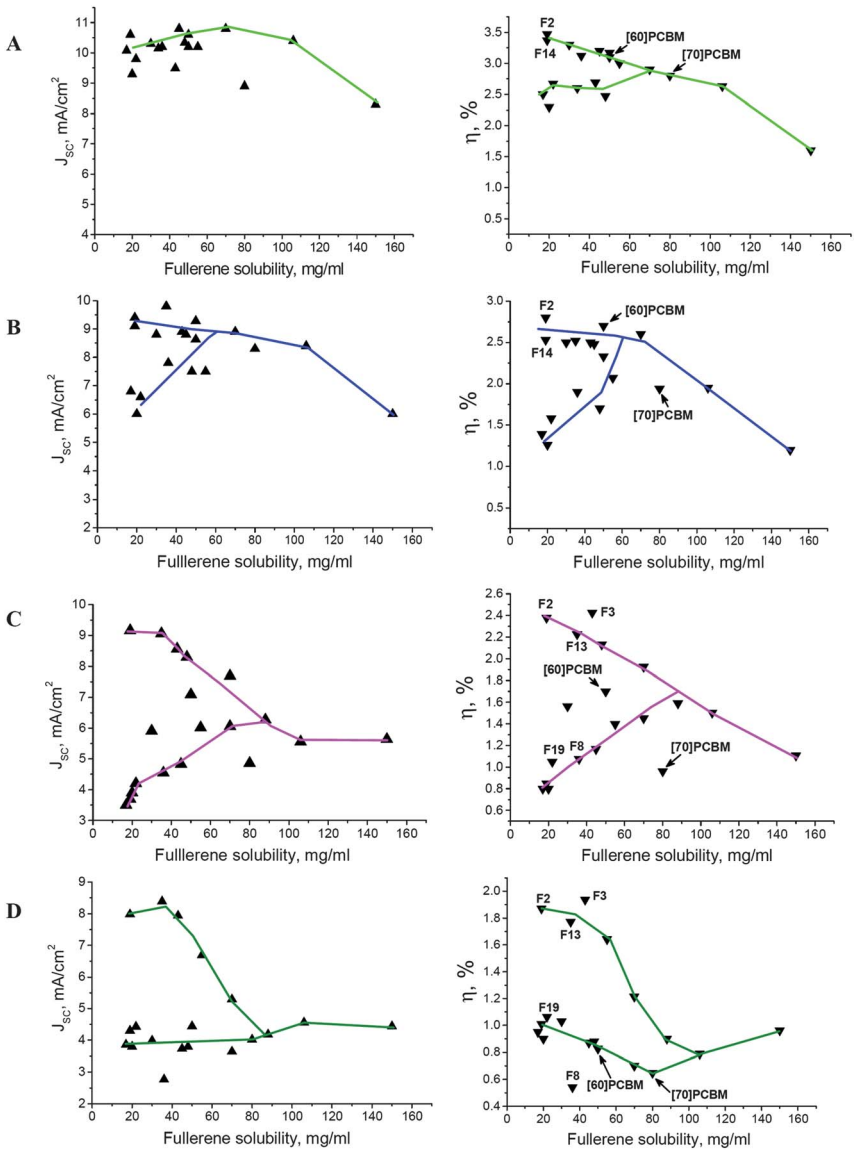

Fig. 5 Short circuit current densities (left) and power conversion efficiencies (right) of photovoltaic devices based on P3PT (A), P3HepT (B), P3OT (C) and P3DT (D) plotted as functions of the solubility of the fullerene component. All lines are provided as guides for the eye.

Variation of the molecular structure of the cyclopropane addend in the fullerene derivatives **F1–F19** affects the tendency of these materials to crystallize and, most probably, also the enthalpy of their crystallization.

When we mix conjugated polymer and fullerene derivative together, the structure of the blend is defined by intermolecular interactions between the fullerene derivative and the polymer. The formation of a homogeneous blend can be expected when fullerene–polymer interactions are stronger compared to fullerene–fullerene and polymer–polymer association (and *vice versa*). Fullerene derivatives (*e.g.* **F8**) which have a strong tendency to crystallization (due to strong fullerene–fullerene intramolecular interactions and other factors) do not mix well with many conjugated polymers thus producing highly inhomogeneous composite films.

To improve the homogeneity of the polymer/fullerene blend one should decrease the tendency of the fullerene derivative to crystallize from solutions which might be achieved by the introduction of some longer or branched alkyl chains. At the same time, the strength of the fullerene–polymer interactions can be increased by using fullerene derivatives bearing relatively long and linear alkyl chains complementary to the ones attached to the polymer backbone.

These considerations are further supported by the AFM images of some fullerene/polymer composites shown in Fig. 6 and S9 (ESI†). Fig. 6 shows AFM topography images for the blends of P3OT and P3DT with three different fullerene derivatives possessing similar solubility (35–43 mg ml^{-1}) and rather different molecular structures. The composites containing fullerene derivative **F8** exhibited characteristic irregularities on the films surface implying rather strong phase separation between the components of the blends. The strong phase separation in the composites **F8**/P3OT and **F8**/P3DT seems to be responsible for their poor photovoltaic performance. In contrast, fullerene derivatives **F3** and **F13** produced rather homogeneous composites yielding reasonably high efficiencies in organic bulk heterojunction solar cells.

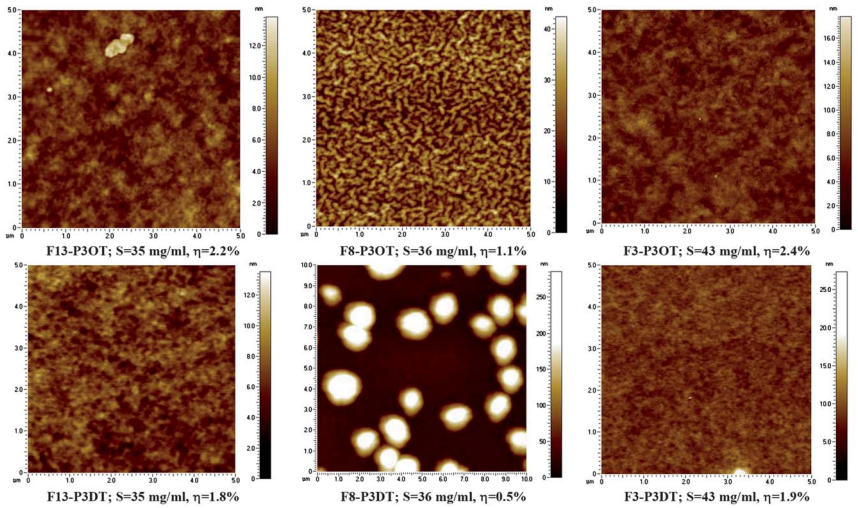

Fig. 6 AFM images of the blends composed of P3OT or P3DT and three different fullerene derivatives with the solubility (*S*) of 35–43 mg ml^{-1} (in chlorobenzene). Composites of the fullerene derivative **F8** exhibit clearly visible irregularities on the film surface implying rather strong phase separation between the components in the blends. This phase separation leads to poor photovoltaic performance of the **F8**/P3OT and **F8**/P3DT composites compared to analogous systems comprising **F3** or **F13**.

Very similar behavior was observed for the fullerene derivatives **F2** (S = 19 mg ml^{-1}) and **F19** (S = 22 mg ml^{-1}). AFM images shown in Fig. S9† prove that **F2** gives smoother (and presumably more homogeneous) blends with **P3ATs** compared to **F19**. Therefore, the composites **F2**/P3OT and **F2**/P3DT outperform significantly analogous systems containing **F19** as a fullerene-based component.

It is worth noting that [60]PCBM (**F1**) and [70]PCBM (**F9**) cannot be considered as the best fullerene-based materials for all different P3ATs. Indeed, [60]PCBM works well with P3HT and P3HepT (Fig. 4 and 5). However, the efficiency of [60]PCBM-based solar cells drops to rather modest level compared to some other fullerene derivatives when P3BT, P3PT, P3OT, P3DT or P3DDT are used as electron donor polymers. At the same time, the devices comprising [70]PCBM as electron acceptor component showed inferior performance in combination with all studied P3ATs (Fig. 5, S7 and S8†).

These examples clearly show that [60]PCBM and [70]PCBM cannot be treated as universal fullerene-based test materials well suitable for every electron donor conjugated polymer. On the contrary, every new polymer seems to require some appropriate fullerene-based counterpart with optimized molecular structure and physical properties (solubility in organic solvents).

5. Solubility and molecular compatibility effects in the blends of fullerene derivatives with some electron donor copolymers

It was shown that molecular structures and the solubility of the fullerene derivatives might be correlated with the morphology and photovoltaic performance of their blends with P3ATs. However, state of the art organic bulk heterojunction solar cells are based on low band gap copolymers that outperform P3ATs significantly.[1–3] Therefore, it is important to check if the general dependences (current density–solubility and efficiency–solubility profiles) revealed for the P3AT-based systems can be applied somehow to the blends comprising other types of conjugated polymers. The copolymers **CP-I** and **CP-II** were selected as model electron donor materials. It should be noted that polymer **CP-I** has a relatively high oxidation potential and therefore it gives open circuit voltages up to 900–1000 mV in organic solar cells.[33] Copolymer **CP-II** is remarkable because of its low band gap allowing potentially for high short circuit current densities in photovoltaic devices.

Limited amounts of the copolymers **CP-I** and **CP-II** available in our studies allowed for evaluation of their photovoltaic performance only using a smaller set of fullerene derivatives consisting of compounds **F1–F13**. The obtained results are shown in Fig. 7. It is seen from this figure that the solubility profiles for both short circuit current density and light power conversion efficiency demonstrate characteristic double-branched shapes very similar to the ones revealed for poly-(3-alkylthiophenes). Due to some fortunate coincidence, [60]PCBM (**F1**) afforded one of the highest power conversion efficiencies in combination with both polymers. However, it was not the case for [70]PCBM (**F9**), which showed quite low performance in combination with **CP-I**. Moreover, both [60]PCBM and [70]PCBM demonstrated quite modest photovoltaic efficiencies in combination with a number of P3ATs (see above) and two PPV-PPE type conjugated copolymers reported by us very recently.[34]

Fig. 7 shows that variation of the fullerene-based counterpart might easily change the photovoltaic performance of **CP-I** and **CP-II** by a factor of 2–4. It is known that many conjugated polymers were discarded as unpromising because they showed *ca.* 2% power conversion efficiency in routine tests in combination with just one fullerene derivative (*e.g.* PCBM). However, exactly the same materials might potentially afford the efficiencies of 4–8% in solar cells (if these are within theoretically allowed values) if appropriate fullerene-based components are provided.

Conclusions

The performed combinatorial study involving 9 different conjugated polymers and 19 different fullerene derivatives

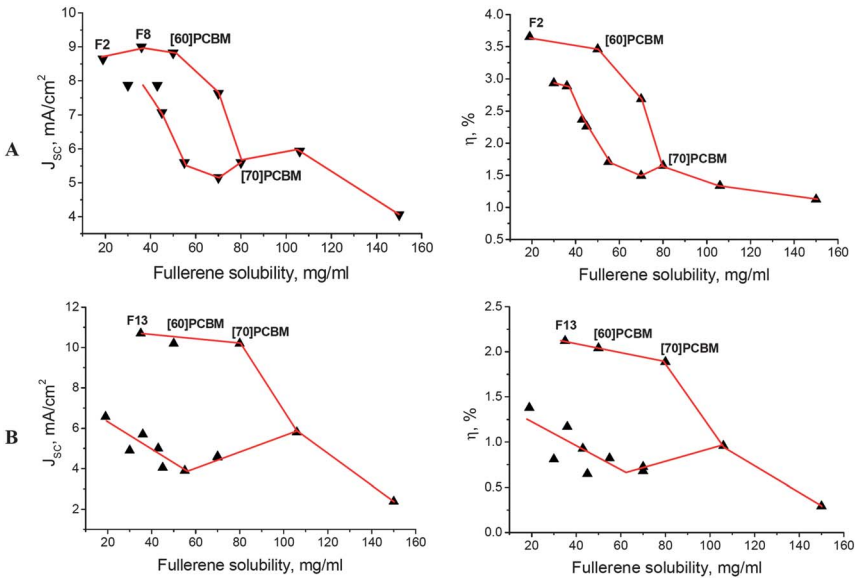

Fig. 7 Short circuit current density (left column) and power conversion efficiency (right column) of solar cells based on the copolymers **CP-I** (raw A) or **CP-II** (raw B) and different fullerene derivatives. The red lines are provided only as guides for the eye.

allowed us to correlate the photovoltaic performance of their bicomponent blends with the solubility and molecular structure peculiarities of the materials.

It was demonstrated that the lengths of the alkyl side chains attached to the polythiophene backbone affect significantly the morphology and photovoltaic performance of their blends with different fullerene derivatives. Polymers bearing normal pentyl (C5), hexyl (C6) and heptyl (C7) side chains produced the most homogeneous composites with the fullerene derivatives and therefore yielded the highest photovoltaic efficiencies. Poly(3-alkylthiophenes) with shorter (butyl, C4) or longer (C8, C10, C12) alkyl side chains showed inferior properties. The observed poor performance of P3BT modified with short alkyl chains (C4) might be associated with the insufficient solubility of this polymer. The presence of long and bulky side chains (P3OT, P3DT, P3DDT) hinders charge transport properties of P3ATs and also might damage some steric and electronic communications between the polymers and the fullerene derivatives that are required for stabilization of the blend morphology and efficient photoinduced charge separation.

The obtained results suggest strongly that some peculiarities of the molecular structures of the fullerene derivatives induce better or worse compatibility of these compounds with the electron donor polymers (P3ATs or conjugated copolymers). At the same time, the side chains attached to the polymer backbone also improve or hinder compatibility of the polymers with a certain fullerene derivative.

Therefore, the morphology and photovoltaic performance of the blends are governed to a large extent by intermolecular interactions between the fullerene derivative and the conjugated polymer counterparts. The solubility of the fullerene derivatives still plays an important role. However, the molecular compatibility effects might be considered as a superior parameter influencing the behavior of the fullerene/polymer composites if the solubility of the fullerene component in chlorobenzene lies in the range of 17–75 mg ml^{-1}.

We note also that the revealed correlations might change significantly when some different solvents (*e.g.* chloroform or 1,2-dichlorobenzene) or processing additives (*e.g.* 1,8-diiodooctane, 1,8-octanedithiol) are applied for the composite film casting. Nevertheless, we believe that general principles, particularly the material solubility and material compatibility effects presented in this work, have to be considered for any fullerene derivative/polymer system regardless of the film processing conditions.

Taking into account the revealed correlations, it was not surprising that conventional fullerene based materials such as [60]PCBM and [70]PCBM showed rather modest photovoltaic performances when studied in combination with a number of conjugated polymers. Every polymer requires its own appropriate fullerene-based counterpart with optimized molecular structure and physical properties (solubility). This is an important observation suggesting the need for revisiting many theoretically promising electron donor copolymers that practically showed power conversion efficiencies of 2–3% with PCBM and consequently were discarded. It has been demonstrated in the present work that replacement of the fullerene counterpart might improve the photovoltaic performance of many conjugated polymers by a factor of 2–4. This means that previously discarded polymers might still give state of the art photovoltaic performances if appropriate fullerene-based counterparts are provided.

Experimental

General

All solvents and reagents were purchased from Sigma-Aldrich or Acros Organics and used as received or purified according to standard procedures. Anhydrous solvents provided by Aldrich were used for deposition of fullerene/polymer blends. Poly-(3-alkylthiophenes) of EE grade were purchased from Rieke Metals company. Molecular weight characteristics and solubility values estimated for investigated P3ATs are given in Table 1.

Table 1 Molecular weight characteristics and solubility values estimated for P3ATs[a]

Polymer	M_w, g mol^{-1}	Solubility in chlorobenzene, mg ml^{-1}
P3BT	57 000	10–25
P3PT	64 000	30–60
P3HT	65 000	60–90
P3HepT	73 000	70–110
P3OT	85 000	80–130
P3DT	79 000	>130
P3DDT	86 000	>130

[a] Conjugated copolymers **CP-I** (M_w = 10 050 g mol^{-1}; PDI = 1.3) and **CP-II** (M_w = 36 300 g mol^{-1}; PDI = 2.3) were synthesized using a combination of the standard procedures previously reported in literature.[35,36] The synthesis of fullerene derivatives was performed according to a previously reported procedure. The experimental details concerning the synthesis of specific compounds may be found in previous publications.

Fabrication of the solar cells

The general procedure used for fabrication of organic bulk heterojunction solar cells was reported previously. Some alterations are described below for certain types of conjugated polymers.

Poly(3-alkylthiophenes) P3ATs. The ratio between the polymer and the fullerene derivative was set constantly equal to 1.6 : 1 for all investigated systems. The solutions were prepared by dissolving P3AT (12 mg) and a fullerene derivative (7.5 mg) in 1 ml of chlorobenzene while stirring the mixture at room temperature for 8–14 h. The spin-coating frequency was set to 800 rpm for the active layer casting regardless of the composition of the blend. Thermal treatment was typically applied to the devices after the deposition of the top aluminium electrodes. The optimal annealing temperatures were found to be different for the systems comprising different P3ATs as shown in Table 2. The post-production treatment regimes presented in Table 2 were kept the same for every series of devices based on a certain P3AT and all nineteen fullerene derivatives investigated in this work. Therefore, there was virtually no variation in the experimental conditions when one fullerene derivative was investigated after the other.

At least two independent batches of photovoltaic devices were fabricated for every bicomponent system to avoid contribution of some stochastic effects appearing particularly during the top electrode deposition. Moreover, every fabricated batch comprised a few reference devices based on the material combination with well established photovoltaic performance (typically, P3HT/[60]PCBM). In the cases when the efficiencies of the devices fabricated in different batches did not agree well with each other or when the reference cells showed lower performance than expected the experiments were reproduced several times until the complete reproducibility was achieved.

We found that optimal device fabrication conditions revealed for the P3AT/[60]PCBM solar cells can be also successfully applied to many other fullerene derivative/P3AT binary systems. Therefore, a replacement of [60]PCBM with other fullerene derivatives does not require significant variation in the blend processing conditions. We performed careful optimization of the component ratio, spin-coating frequency and post-production treatment regimes for the **F2**/P3AT, **F11**/P3AT, **F5**/P3AT and **F7**/P3AT composite systems (data not shown). The resulting improvement of the solar cell performance was rather minor (5–10% of the initial value) compared to the effects observed while replacing one fullerene derivative with another. Therefore, the processing of different fullerene derivatives under fully identical conditions produced results which seem to reflect with good accuracy the real photovoltaic performance of every studied bicomponent fullerene derivative/P3AT system.

Photovoltaic devices based on the copolymer CP-I. Conjugated polymer **CP-I** (5 mg) and the fullerene derivative (20 mg) were dissolved together in 1 ml of chlorobenzene while stirring at 50 °C for 12 h. The warm solution was filtered through a PTFE 0.45 μm syringe filter, heated back up to 50–60 °C and subjected to spin-coating at 800 rpm on the top of the annealed PEDOT:PSS films deposited on patterned ITO electrodes (see ref. 22 for general description of the substrate preparation procedure). The obtained films were transferred immediately into a vacuum chamber integrated inside an MBraum glovebox and pumped down for *ca.* 1 h until the pressure dropped below 4×10^{-6} mbar. The top electrode comprising 0.7 nm of LiF and 100 nm of Al was deposited by thermal evaporation. The finalized devices were immediately subjected to the *I–V* and IPCE characterisation.

Photovoltaic devices based on the copolymer CP-II. Conjugated polymer **CP-II** (10 mg) and the fullerene derivative (20 mg) were dissolved together in 1 ml of chlorobenzene while stirring at room temperature overnight. The prepared solution was filtered through a PTFE 0.45 μm syringe filter before spin-coating. The fullerene derivative/polymer blends were deposited at the frequency of 800 rpm and then were dried in vacuum for *ca.* 1 h. The top aluminium electrode (100 nm) was deposited by thermal evaporation at a pressure of 2–4 $\times$ 10^{-6} mbar. The devices were annealed at 143 °C for 3 minutes directly before characterization.

Characterisation of the solar cells

The current–voltage (*I–V*) characteristics of the devices were obtained in the dark and under simulated 100 mW cm^{-2} AM1.5 solar irradiation provided by a KHS Steuernagel solar simulator.

Table 2 Optimal post-production treatment regimes applied to the solar cells based on P3ATs/fullerene derivative composites

Polymer	Annealing temperature, °C	Annealing time, min	Polymer	Annealing temperature °C	Annealing time, min
P3BT	110	3	P3OT	130	3
P3PT	155	3	P3DT	110	3
P3HT	155	3	P3DDT	No annealing	
P3HepT	140	2			

The intensity of the illumination was checked every time before the measurements using a calibrated silicon diode with known spectral response. All data given in this paper were not corrected for the mismatch between the solar simulator illumination and the AM1.5 spectrum. The performances of the best cells were cross-checked using two different solar simulators at two independent laboratories (LIOS, Linz, Austria and IPCP RAS, Chernogolovka, Russia) that provided very similar results. The photocurrent spectra were measured with a SRS 830 lock-in amplifier using the monochromated light from a 75 W Xe lamp as excitation source. Integration of the experimental IPCE spectra over the real AM1.5 irradiation spectrum was used to check the short circuit current densities obtained from the *I–V* curves. The relative discrepancy between the values was within 7–12% (2–3% for solar cells based on **CP-II**), which might be associated with the spectral mismatch of the solar simulator irradiation and/or with a nonlinear light intensity dependence of the photocurrent response of the devices.

AFM measurements

The AFM characterization of the fullerene derivative/polymer composites was carried out using the best performing photovoltaic devices. The images were taken from the film areas closely adjacent to the device top electrode. Such characterisation allowed us to exclude any kind of stochastic effects influencing the blend morphology. Therefore, the AFM images presented in this work for every bicomponent fullerene derivative/polymer system can be directly correlated with its photovoltaic performance.

Acknowledgements

The authors acknowledge financial support provided by the Russian Ministry of Science and Education in the framework of the contract No. 02.740.11.0749 and the Federal Program "Priority Directions of the Research and Development of the Scientific and Technological Infrastructure in Russia in 2007–2013", the Russian Foundation for Basic Research (10-03-00443a and 10-03-01009a) and the Russian President Science Foundation (MK-4916.2011.3 and MK 1528.2011.3).

References

1 R. F. Service, *Science*, 2011, **332**, 293.
2 Y.-J. Cheng, S.-H. Yang and C.-S. Hsu, *Chem. Rev.*, 2009, **109**, 5868.
3 J. Chen and Y. Cao, *Acc. Chem. Res.*, 2009, **42**, 1709.
4 M. C. Scharber, D. Muhlbacher, M. Koppe, P. Denk, C. Waldauf, A. J. Heeger and C. J. Brabec, *Adv. Mater.*, 2006, **18**, 789.
5 D. Gendron and M. Leclerc, *Energy Environ. Sci.*, 2011, **4**, 1225.
6 J. M. Szarko, J. Guo, B. S. Rolczynski and L. X. Chen, *J. Mater. Chem.*, 2011, **21**, 7849.
7 J. C. Bijleveld, M. Shahid, J. Gilot, M. M. Wienk and R. A. J. Janssen, *Adv. Funct. Mater.*, 2009, **19**, 3262.
8 S. Wakim, S. Beaupre, N. Blouin, B.-R. Aich, S. Rodman, R. Gaudiana, Y. Tao and M. Leclerc, *J. Mater. Chem.*, 2009, **19**, 5351.
9 N. Blouin, A. Michaud, D. Gendron, S. Wakim, E. Blair, R. Neagu-Plesu, M. Belletete, G. Durocher, Y. Tao and M. Leclerc, *J. Am. Chem. Soc.*, 2008, **130**, 732.
10 J. L. Delgado, P.-A. Bouit, S. Filippone, M. A. Herranz and N. Martin, *Chem. Commun.*, 2010, **46**, 4853.
11 F. G. Brunetti, R. Kumar and F. Wudl, *J. Mater. Chem.*, 2010, **20**, 2934.
12 F. B. Kooistra, J. Knol, F. Kastenberg, L. M. Popescu, W. J. H. Verhees, J. M. Kroon and J. C. Hummelen, *Org. Lett.*, 2007, **9**, 551.
13 Y. He, H. Y. Chen, J. Hou and Y. Li, *J. Am. Chem. Soc.*, 2010, **132**, 1377.
14 M. Lenes, G.-J. A. H. Wetzelaer, F. B. Kooistra, S. C. Veenstra, J. C. Hummelen and P. W. M. Blom, *Adv. Mater.*, 2008, **20**, 2116.
15 P. A. Troshin, E. A. Khakina, M. Egginger, A. E. Goryachev, S. I. Troyanov, A. Fuchsbauer, A. S. Peregudov, R. N. Lyubovskaya, V. F. Razumov and N. S. Sariciftci, *ChemSusChem*, 2010, **3**, 356.
16 P. A. Troshin, R. Koeppe, D. K. Susarova, N. V. Polyakova, A. S. Peregudov, V. F. Razumov, N. S. Sariciftci and R. N. Lyubovskaya, *J. Mater. Chem.*, 2009, **19**, 7738.
17 C. Yang, J. Y. Kim, S. Cho, J. K. Lee, A. J. Heeger and F. Wudl, *J. Am. Chem. Soc.*, 2008, **130**, 6444.
18 J. L. Delgado, E. Espíldora, M. Liedtke, A. Sperlich, D. Rauh, A. Baumann, C. Deibel, V. Dyakonov and N. Martín, *Chem.–Eur. J.*, 2009, **15**, 13474.
19 R. B. Ross, C. M. Cardona, D. M. Guldi, S. G. Sankaranarayanan, M. O. Reese, N. Kopidakis, J. Peet, B. Walker, G. C. Bazan, E. Van Keuren, B. C. Holloway and M. Drees, *Nat. Mater.*, 2009, **8**, 208.
20 J. C. Hummelen, B. W. Knight, F. Lepeq, F. Wudl, J. Yao and C. L. Wilkins, *J. Org. Chem.*, 1995, **60**, 532.
21 M. M. Wienk, J. M. Kroon, W. J. H. Verhees, J. Knol, J. C. Hummelen, P. A. van Hall and R. A. J. Janssen, *Angew. Chem., Int. Ed.*, 2003, **42**, 3371.
22 P. A. Troshin, H. Hoppe, J. Renz, M. Egginger, J. Yu. Mayorova, A. E. Goryachev, A. S. Peregudov, R. N. Lyubovskaya, G. Gobsch, N. S. Sariciftci and V. F. Razumov, *Adv. Funct. Mater.*, 2009, **19**, 779.
23 J. Y. Mayorova, S. L. Nikitenko, P. A. Troshin, S. M. Peregudova, A. S. Peregudov, M. G. Kaplunov and R. N. Lyubovskaya, *Mendeleev Commun.*, 2007, **17**, 175.
24 P. A. Troshin, H. Hoppe, A. S. Peregudov, M. Egginger, S. Shokhovets, G. Gobsch, N. S. Sariciftci and V. F. Razumov, *ChemSusChem*, 2011, **4**, 119.
25 V. A. Kostyanovsky, D. K. Susarova, A. S. Peregudov and P. A. Troshin, *Thin Solid Films*, 2011, **519**, 4119.
26 L. H. Nguyen, H. Hoppe, T. Erb, S. Guenes, G. Gobsch and N. S. Sariciftci, *Adv. Funct. Mater.*, 2007, **17**, 1071.
27 A. Gadisa, W. D. Oosterbaan, K. Vandewal, J.-C. Bolsee, S. Bertho, J. D'Haen, L. Lutsen, D. Vanderzande and J. V. Manca, *Adv. Funct. Mater.*, 2009, **19**, 3300.
28 P.-T. Wu, H. Xin, F. S. Kim, G. Ren and S. A. Jenekhe, *Macromolecules*, 2009, **42**, 8817.
29 K. Vandewal, W. D. Oosterbaan, S. Bertho, V. Vrindts, A. Gadisa, L. Lutsen, D. Vanderzande and J. V. Manca, *Appl. Phys. Lett.*, 2009, **95**, 123303.
30 W. D. Oosterbaan, V. Vrindts, S. Berson, S. Guillerez, O. Douhéret, B. Ruttens, J. D'Haen, P. Adriaensens, J. Manca, L. Lutsen and D. Vanderzande, *J. Mater. Chem.*, 2009, **19**, 5424.
31 C. J. Brabec, A. Cravino, D. Meissner, N. S. Sariciftci, T. Fromherz, M. T. Rispens, L. Sanchez and J. C. Hummelen, *Adv. Funct. Mater.*, 2001, **11**, 374.
32 T. Chen, X. Wu and R. D. Rieke, *J. Am. Chem. Soc.*, 1995, **117**, 233; K. Yazawa, Y. Inoue, T. Yamamoto and N. Asakawa, *Phys. Rev. B: Condens. Matter Mater. Phys.*, 2006, **74**, 094204.
33 F. Zhang, K. G. Jespersen, C. Björström, M. Svensson, M. R. Andersson, V. Sundström, K. Magnusson, E. Moons, A. Yartsev and O. Inganäs, *Adv. Funct. Mater.*, 2006, **16**, 667.
34 D. K. Susarova, E. A. Khakina, P. A. Troshin, A. E. Goryachev, N. S. Sariciftci, V. F. Razumov and D. A. M. Egbe, *J. Mater. Chem.*, 2011, **21**, 2356; P. A. Troshin, O. A. Mukhacheva, O. Usluer, S. Rathgeber, A. E. Goryachev, A. V. Akkuratov, D. K. Susarova, N. S. Sariciftci, V. F. Razumov and D. A. M. Egbe, *Adv. Energy Mater.*, 2012, DOI: 10.1002/aenm.201200118.
35 M. Svensson, F. Zhang, S. C. Veenstra, W. J. H. Verhees, J. C. Hummelen, J. M. Kroon, O. Inganas and M. Andersson, *Adv. Mater.*, 2003, **15**, 988.
36 A. J. Moulé, A. Tsami, T. W. Bünnagel, M. Forster, N. M. Kronenberg, M. Scharber, M. Koppe, M. Morana, C. J. Brabec, K. Meerholz and U. Scherf, *Chem. Mater.*, 2008, **20**, 4045.